Supplementary Information for:

Micro-flower changing to nano-bundle aggregates by translocation of the sugar moiety in Janus TA nucleosides

Hang Zhao[a,b‡], Shiliang He[a‡], Mingli Yang[c], Xiurong Guo[a], Guang Xin[a], Chaoyang Zhang[b], Ling Ye[b], Liangyin Chu[b], Zhihua Xing[a], Wen Huang[a], Qianming Chen[b]* and Yang He[a]**

[a] *Laboratory of Ethnopharmacology, Institute for Nanobiomedical Technology and Membrane Biology, Regenerative Medicine Research Center, West China Hospital, West China Medical School, Sichuan University, Chengdu 610041, China;* [b] *State Key Laboratory of Oral Diseases, West China Hospital of Stomatology, Sichuan University, Chengdu 610041, China;* [c] *Institute of Atomic and Molecular Physics, Sichuan University, Chengdu 610065, China.*

Experimental section

All chemicals were commercially available. The solvents and reagents were analytic pure. Solvents 1, 2-dichloroethane and acetonitrile were purified by distilling from P_2O_5. Pyridine was dried by treating with calcium hydride. Thin-layer chromatography (TLC) was performed on aluminium sheet covered with silica gel 60 F254 (0.2 mm, Merck, Germany). Flash column chromatography (FC): silica gel 60 (Haiyang chemical company, P. R. China) at 0.4 bar. NMR spectra were recorded on a AV II (Bruker, Germany) spectrometer at 400 MHz and 600 MHz, the δ values in ppm are relative to Me_4Si as internal standard; High resolution mass spectra were measured with mass analyzer (Q-TOF, Bruker, Germany); The UV absorption spectra were recorded on a DU-800 spectrophotometer (Beckman, US), λ_{max} in nm, ε in dm^3 mol^{-1} cm^{-1}.

Chemical synthesis:

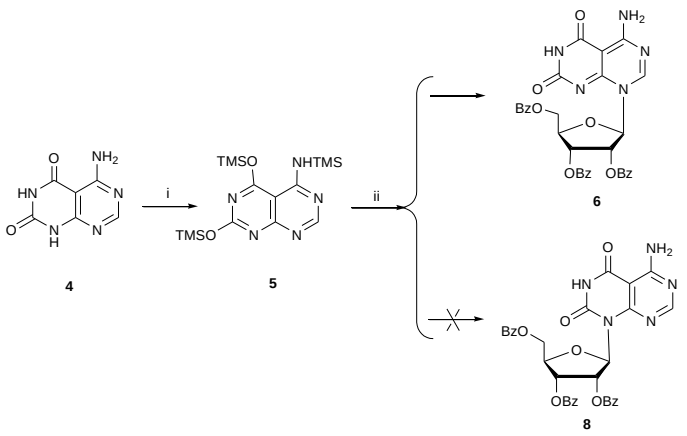

Scheme S1. The failed synthesis routes of the J-TA nucleoside analogue: i). HMDS, TMSCl, reflux; ii). Different Friedel-Crafts catalysts ($SnCl_4$, TMSOTf), solvents ($ClCH_2CH_2Cl$, CH_3CN and $CHCl_3$) and reaction times (1h, 2h, 5h, 1d and 3d) were investigated.

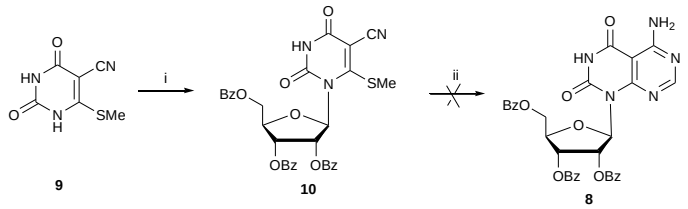

Scheme S2. The failed synthesis routes of the J-TA nucleoside analogue: i). HMDS, TMSCl, reflux, dry acetonitrile, $SnCl_4$, 80%; ii). Formamide, 180℃, 8 h.

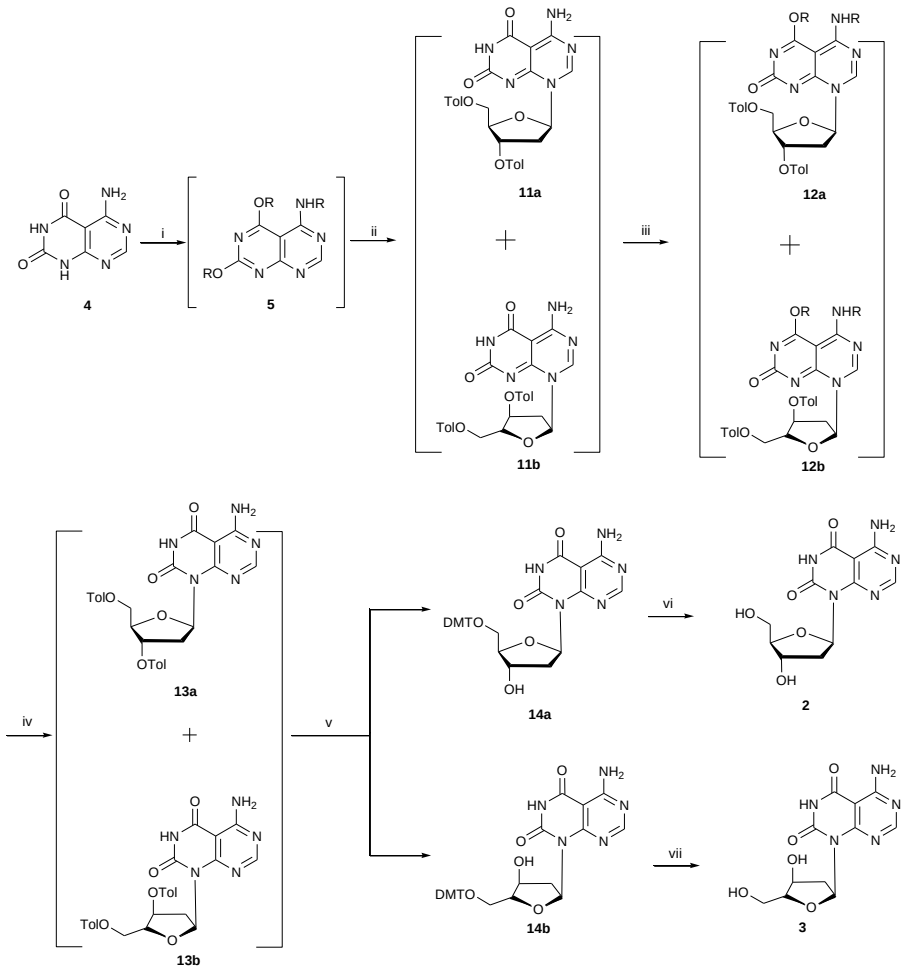

Scheme S3. Synthesis of the J-TA 2'-deoxyribosenucleoside (**2**) and (**3**): R=TMS; i). HMDS, TMSCl, reflux; ii). $ClCH_2CH_2Cl$:CH_3CN (1:1), TMSOTf, r.t., 1 h; iii). HMDS, xylene, reflux; iv). Dry acetonitrile, TMSOTf, 75℃, 2 h; v). 0.2 M NaOMe, reflux; dry pyridine, DMT-Cl, DMAP, overnight at r.t.; vi), vii). 1.5% of DCA in CH_2Cl_2, r.t..

1-(2, 3, 5-tri-O-benzoyl-β-D-ribofuranosyl)-5-cyano-6-methylthio-pyrimidine-2, 4(1H, 3H)-dione (10)

Compound **9** (2.00 g, 10.92 mmol) was suspended in hexamethyldisilazane (HMDS, 150 mL). After the mixture being stirred at 140 ºC for 3 min, the trimethylsiyl chloride (TMSCl, 2 mL) was added. The mixture was stirred under refluxing for about 10 h until the mixture turned clear. Then, the solution was evaporated to remove excess HMDS and the silylated base was obtained and immediately used without further purification. At room temperature, to this silylated base residue was added dry acetonitrile (200 mL) followed by adding 1-O-acetyl-2, 3,

5-tri-O-benzoyl-β-D-ribofuranose (4.80 g, 9.52 mmol). This mixture was cooled to 0 ºC and $SnCl_4$ (2 mL) was added as catalyst. After the mist vanishing, the reaction was brought to room temperature and the stirring was continued for 1 h. Then, saturated $NaHCO_3$ aqueous solution (100 mL) was added at 0 ºC to quench the reaction. Next, 300 mL CH_2Cl_2 was added. The organic phase was collected and dried with anhydrous Na_2SO_4. After the evaporation of the CH_2Cl_2, the residue was applied to FC (CH_2Cl_2: methanol = 98:2) and compound **10** was obtained as colorless powder (5.50 g, 80%). ^{1}H NMR (400 MHz, DMSO-d_6) δ (ppm): 2.74 (3H, s, -SMe), 4.5-4.7 (3H, m, 5'-CH_2 and 4'–CH), 6.09-6.14 (2H, m, 2'-CH and 3'-CH), 6.49 (1H, d, *J* =1.6 Hz, 1'-CH), 7.32-8.0 (15H, m, -C_6H_5); ^{13}C NMR (100 MHz, DMSO-d_6) δ (ppm): 14.35, 63.19, 69.94, 73.55, 78.04, 84.41, 85.62, 85.65, 114.07, 128.53, 128.62, 128.77, 129.19, 129.35, 133.43, 133.68, 133.88, 149.07, 158.95, 164.52, 164.71, 165.47, 166.37; UV(EtOH): λ_{max} (ε): 204 (26651); 229 (55927); 301 (13423); TLC (CH_2Cl_2: MeOH = 99:1): R_f = 0.2; HRMS (ESI) calculated for ($M+Na^+$)/z: 650.121, found: 650.1207.

1-(2,3,5-tri-O-benzoyl-β-D-ribofuranosyl)-5-amino-pyrimido[4,5-*d*]pyrimidine-2, 4(1H, 3H)-dione (8)

To a solution of compound **6** (1.70 g, 2.73 mmol) in excess of hexamethyldisilazane (HMDS, 100 mL) was added the xylene (30 mL). The mixture was heated in an oil bath to 140℃ with exclusion of moisture. The reaction was carried out at 140℃ for about 1 h until the mixture turned clear solution. Then, the excess HMDS and xylene were removed under reduced pressure to give a syrup which was used for next step immediately without purification. Dry acetonitrile (100 mL) and TMSOTf : $ClCH_2CH_2Cl$ (1:1, 300 μL) was added to this syrup at room temperature. Then, the reaction mixture was stirred at 75℃ for about 2 h. The reaction was diluted with DCM, followed by washing with $NaHCO_3$. The organic layer was dried with anhydrous Na_2SO_4 and evaporated. The resulting crude product was applied to FC (CH_2Cl_2: MeOH = 99:1-97:3) and the pure product **8** was obtained as colorless powder (867 mg, 51%). ^{1}H NMR (600 MHz, DMSO-d_6) δ (ppm): 4.52-4.55

(1H, m, 4'-CH), 4.65-4.70 (2H, m, 5'-CH_2), 6.13-6.19 (2H, m, 2'-CH and 3'-CH), 6.58 (1H, s, 1'-CH), 7.34-8.0 (15H, m, -C_6H_5), 8.14-8.41 (2H, m, -NH_2), 8.29 (1H, s, 7-CH), 12.19 (1H, s, -NH); ^{13}C NMR (100 MHz, DMSO-d_6) δ (ppm): 73.70, 77.86, 128.55, 128.64, 128.78, 128.83, 129.19, 129.26, 129.29, 129.33, 129.42, 129.47, 133.44, 133.69, 133.87, 157.43, 157.46, 157.47, 162.14, 162.55, 164.54, 164.74, 165.44, 165.47, 170.26; UV(EtOH): λ_{max} (ε): 202 (7714); 227 (5386); TLC (CH_2Cl_2 : MeOH = 99:2): R_f = 0.2; HRMS (ESI) calculated for ($M+H^+$)/z: 624.1731, found: 624.1735.

1-(β-D-ribofuranosyl)-5-amino-pyrimido[4,5-*d*]pyrimidine-2,4(1H, 3H)-dione (1)

Compound **8** (170 mg, 0.27 mmol) was dissolved in 0.5 M NaOMe/MeOH (15 mL), and the solution was refluxed at 75℃ for about 20 min. After cooling to room temperature, the solution was neutralized with diluted acetic acid to pH 6.5 and precipitate was formed. After filtration the precipitate was washed with methanol (3 × 5 mL) and water (1 × 5 mL). Target compound **1** was obtained as white powder by vacuum drying (70 mg, 82%). ^{1}H NMR (600 MHz, DMSO-d_6) δ (ppm): 3.18 (1H, s, 3'-CH), 3.44-3.47 (1H, m, 4'-CH), 3.61-3.72 (4H, m, 5'-CH_2, 2'-CH and 5'-OH), 4.17 (1H, t, *J* =6 Hz, 3'-OH), 4.52-4.54 (1H, q, *J* =3.6 Hz, 2'-OH), 6.17 (1H, d, *J* =3.6 Hz, 1'-CH), 7.79-8.19 (2H, m, -NH_2), 8.14 (1H, s, 7-CH); ^{13}C NMR (150 MHz, DMSO-d_6) δ (ppm): 62.99, 65.71, 67.59, 71.85, 84.77, 90.43, 161.46, 163.46, 166.23, 166.10, 175.47; UV(H_2O): λ_{max} (ε): 227 (10412); 289 (1777); HRMS (ESI) calculated for ($M+Na^+$)/z: 334.0764, found: 334.0766.

1-[2-deoxy-3,5-di-O-(p-toluoyl)-β-D-ribofuranosyl]-5-amino-pyrimido[4,5-*d*]pyrimidine-2,4(1H,3H)-dione (13a)

1-[2-deoxy-3,5-di-O-(p-toluoyl)-*α*-D-ribofuranosyl]-5-amino-pyrimido[4,5-*d*]pyrimidine-2,4(1H, 3H)-dione (13b)

Compound **11** (1.00 g, 1.78 mmol) was suspended in HMDS (50 mL) and the mixture was stirred at 140 ºC for about 5 min, then xylene (15 mL) was added. The

mixture was stirred under refluxing for about 1 h until turned clear, and excess of HMDS and xylene were removed by evaporation. Then, the resulting silylated intermediates (**12a, b**) were directly suspended in 50 mL anhydrous acetonitrile. To this suspension, TMSOTf : $ClCH_2CH_2Cl$ (1:1, 200 μL) was added and the reaction was carried at 75℃ for almost 2 h until the starting material disappeared (monitored by TLC, CH_2Cl_2: MeOH, 95:5). Then, the resulting mixture was diluted with CH_2Cl_2, washed with saturated $NaHCO_3$ aqueous solution. The combined organic layers were dried with anhydrous sodium sulfate and concentrated. Purification of the resulting solid material by FC (CH_2Cl_2: MeOH = 99:1-97:3) afforded 400 mg of compound **13a** and **13b** (40%) as white powder.

1-[2-Deoxy-5-O-(4,4'-dimethoxytrityl)-β-D-ribofuranosyl]-5-amino-pyrimido[4,5-*d*]pyrimidine-2,4(1H, 3H)-dione (14a)

1-[2-Deoxy-5-O-(4,4'-dimethoxytrityl)-α-D-ribofuranosyl]-5-amino-pyrimido[4,5-*d*]pyrimidine-2,4(1H, 3H)-dione (14b)

Compounds **13a** and **13b** (400 mg, 0.75 mmol) were suspended in 0.2 M NaOMe/MeOH (20 mL), the suspension was stirred under refluxing until **13a** and **13b** disappeared (monitored by TLC, CH_2Cl_2: MeOH, 95:5). Then the solution was neutralized with diluted acetic acid to pH 6.5. The resulting precipitate was filtered, washed with methanol (3×10 mL) and water (1×10 mL). These anomeric mixtures of free nucleosides (110 mg) were coevaporated with freshly pyridine (3×10 mL) and redissolved in dry pyridine (5 mL). To this solution, 4, 4-dimethoxytrityl chloride (150 mg, 0.45 mmol) and 4-dimethylaminopyridine (9 mg, 0.45 mmol) was added. The reaction solution was stirred at room temperature overnight. The reaction was quenched by adding 10 mL 5% aqueous solution of sodium bicarbonate at 0℃. The mixture of reaction was extracted with ethyl acetate (3×10 mL), the organic layer was dried with anhydrous Na_2SO_4 and evaporated to get crude product. The separation of **14a** and **14b** was achieved by FC (CH_2Cl_2 : MeOH = 99:1-98:2).

For product **14a** (100 mg, 45%); ^{1}H NMR (400 MHz, DMSO-d_6) δ (ppm): 2.35-2.39 (1H, m, 2'-CH), 2.57-2.63 (1H, m, 2'-CH), 2.94-3.19 (2H, m, 5'-CH_2), 3.74 (6H, s, -OMe), 4.08 (1H, t, 3'-CH), 4.31-4.35 (1H, m, 4'-CH), 5.23-5.33 (1H, m, 3'-OH), 6.55 (1H, t, *J* =8 Hz, 1'-CH), 6.88-7.41 (13H, m, -C_6H_4 and -C_6H_5), 8.24-8.29 (2H, m, -NH_2), 8.27 (1H, s, 7-CH), 11.95 (1H, s, -NH); ^{13}C NMR (100 MHz, DMSO-d_6) δ (ppm): 45.38, 52.0, 55.0, 64.21, 71.12, 81.13, 83.53, 85.22, 89.15, 113.14, 126.57, 127.71, 127.78, 129.69, 135.67, 135.71, 144.98, 149.72, 157.15, 157.99, 161.46, 162.16, 163.06; UV(EtOH): λ_{max}(ε): 206 (25000); 229 (17000); 273 (3200); TLC(CH_2Cl_2): R_f = 0.2; HRMS (ESI) calculated for ($M+Na^+$)/z: 620.2121, found: 620.2109;

For product **14b** (80 mg, 36%); ^{1}H NMR (400 MHz, DMSO -d_6) δ (ppm): 2.03-2.09 (1H, m, 2'-CH), 2.63-2.69 (1H, m, 2'-CH), 3.08-3.28 (2H, m, 5'-CH_2), 3.69 (3H, s, -OMe), 3.72 (3H, s, -OMe), 3.84-3.87 (1H, m, 3'-CH), 4.31-4.32 (1H, m, 4'-H), 5.13-5.14 (1H, m, 3'-OH), 6.61-6.65 (1H, dd, *J* =4 Hz, 1'-CH), 6.79-7.40 (13H, m, -C_6H_4 and -C_6H_5), 8.12-8.27 (2H, m, -NH_2), 8.26 (1H, s, 7-CH), 10.91 (1H, s, -NH); ^{13}C NMR (100 MHz, DMSO-d_6) δ (ppm): 45.37, 54.91, 54.95, 64.59, 71.16, 80.84, 85.22, 85.54, 88.94, 112.94, 113.0, 126.50, 127.62, 127.75, 129.64, 129.76, 129.81, 135.78, 145.12, 149.40, 157.11, 157.13, 157.89, 157.96, 161.49, 162.17, 162.81; UV(EtOH): λ_{max} (ε): 229 (38758); 273 (7143); TLC(CH_2Cl_2): R_f = 0.2; HRMS (ESI) calculated for ($M+Na^+$)/z: 620.2121, found: 620.2113.

1-(2-deoxy-β-D-ribofuranosyl)-5-amino-pyrimido[4, 5-*d*]pyrimi- dine-2, 4(1H, 3H)-dione (2)

Compound **14a** (100 mg, 0.17 mmol) was dissolved in 1.5% of DCA in CH_2Cl_2 (2 mL), the reaction mixture was stirred at r.t. for about 2 min. When compound **14a** disappeared (monitored by TLC, CH_2Cl_2 : MeOH, 12:1), triethylamine was added to neutralize the reaction mixture. Then the reaction mixture was filtered and the precipitate was washed with CH_2Cl_2 (3 × 5 mL) and acetone (3 × 5 mL). After vacuum drying, compound **2** (25 mg, 50%) was obtained as a white powder. ^{1}H NMR

(400 MHz, DMSO-d_6) δ (ppm): 2.31-2.38 (1H, m, 2'-CH), 2.51-2.63 (1H, m, 2'-CH), 3.36-3.60 (2H, m, 5'-CH_2), 4.07-4.14 (2H, m, 3'-CH and 4'-CH), 4.61-4.63 (1H, t, *J* =5.2 Hz, 5'-OH), 5.16-5.18 (1H, d, *J* =2.4 Hz, 3'-OH), 6.48-6.50 (1H, t, *J* = 7.6 Hz, 1'-CH), 8.22-8.23 (2H, d, *J* = 5.2 Hz, -NH_2), 8.25 (1H, s, 7-CH), 11.89-11.90 (1H, d, *J* = 2.4 Hz, -NH); ^{13}C NMR (100 MHz, DMSO-d_6) δ (ppm): 36.39, 61.81, 70.89, 81.45, 86.06, 89.56, 150.26, 157.68, 161.95, 162.66, 163.56; UV(H_2O): λ_{max}(ε): 227 (10000); 289 (1559); HRMS (ESI) calculated for ($M+Na^+$)/z: 318.0815, found: 318.0807.

1-(2-deoxy-α-D-ribofuranosyl)-5-amino-pyrimido[4, 5-*d*]pyrimi-dine-2, 4(1H, 3H)-dione (3)

The deprotection of **14b** (80 mg) was carried out in the same way as described for **14a**, which afforded compound **3** (20 mg, 50%) as white precipitate. ^{1}H NMR (400 MHz, DMSO-d_6) δ (ppm): 1.94-2.01 (1H, m, 2'-CH), 2.68-2.77 (1H, m, 2'-CH), 3.46-3.50 (1H, m, 4'-CH), 3.59-3.68 (2H, m, 5'-CH_2), 4.30-4.34 (1H, dd, *J* = 5.2 Hz, 3'-CH), 4.56-4.58 (1H, t, *J* = 5.6 Hz, 5'-OH), 5.10-5.12 (1H, d, *J* = 4.8 Hz, 3'-OH), 6.55-6.59 (1H, dd, *J* =6 Hz, 1'-CH), 8.18-8.19 (1H, d, *J* =2.4 Hz, -NH_2), 8.25 (1H, s, 7-CH), 8.26-8.27 (1H, d, *J* = 3.2 Hz, -NH_2), 11.84-11.85 (1H, d, *J* = 5.6 Hz, -NH); ^{13}C NMR (100 MHz, DMSO-d_6) δ (ppm): 37.12, 62.74, 71.51, 81.45, 87.89, 89.44, 149.99, 157.62, 161.99, 162.65, 163.43; UV(H_2O): λ_{max} (ε): 227 (5500); 289 (1431); HRMS (ESI) calculated for ($M+Na^+$)/z: 318.0815, found: 318.0805.

Computational details

The initial structures were constructed by linking the J-TA nucleoside monomers through hydrogen bonds (HBs). The sugar rings were replaced with methyl groups for simplicity. All the geometries were optimized at density functional theory level with M062X/6-31G(d,p)[S1] as implemented in Gaussian program[S2]. No symmetry constraint was imposed during the geometry optimization. The polarized continuum model (PCM) [S3] was used to model the solvent effect (water, ε = 78). Basis set superposition errors were corrected with the counterpoise[S4] method. The interaction energy (E_{int})

was defined as $E_{int} = mE_1 - E_m$ where m is the number of molecules in the system. The condensed nucleophilic Fukui functions were computed with a numerical differential method and were used to estimate the reactivity of reaction intermediates. The calculations for the stacking of six-membered J-TA nucleosides up to n = 11 or 12 layers were performed with ff03 force-field[S5] implemented in Amber package[S6]. The structures were fully relaxed after assembling the layers together.

NMR spectra

NMR spectra: AV II spectrometers (Bruker, Germany) at 600 MHz for HMBC, HMQC and VT-NMR, the values in ppm relative to Me_4Si as internal standard; Compounds **1-3** were dissolved in d_6-DMSO (6 mg mL^{-1}).

SEM Imaging

SEM was performed using a high resolution INSPECT F50. All SEM images were obtained without staining. Samples were prepared by dissolving compound **1-3** and J-AT (0.2 mg mL^{-1}) in H_2O. The solutions were heated to ~100°C and allowed to cool to room temperature for ~48 h.

AFM Imaging

AFM measurements were performed in tapping mode (TM–AFM) at amplitude setpoint of 1 V using SPI4000 (Seiko Instruments, Chiba, Japan). Soft silicon cantilevers were chosen (SI-DF2000, K-A102001604, Japan) with spring constant of 5 N/m. Clean mica substrates (1×1 cm^2) were prepared and 5 µL of the RNT samples (0.2 mg mL^{-1} in H_2O) were deposited onto a freshly cleaved mica surface. The mica surface with the adsorbed samples was then dried in air and imaged immediately.

TEM Imaging

TEM images were recorded on a Tecnai G^2 F_{20} microscope operated at 200 KV, 5 µL of each solution were placed on micro ultra-thin carbon coated TEM grid for 1 min before excess material was blotted with filter paper. All the samples were air-dried for 2 h at room temperature. The grids were stained with an aqueous solution of uranyl acetate (2% w/v) for 40 s and dried at room temperature before imaging.

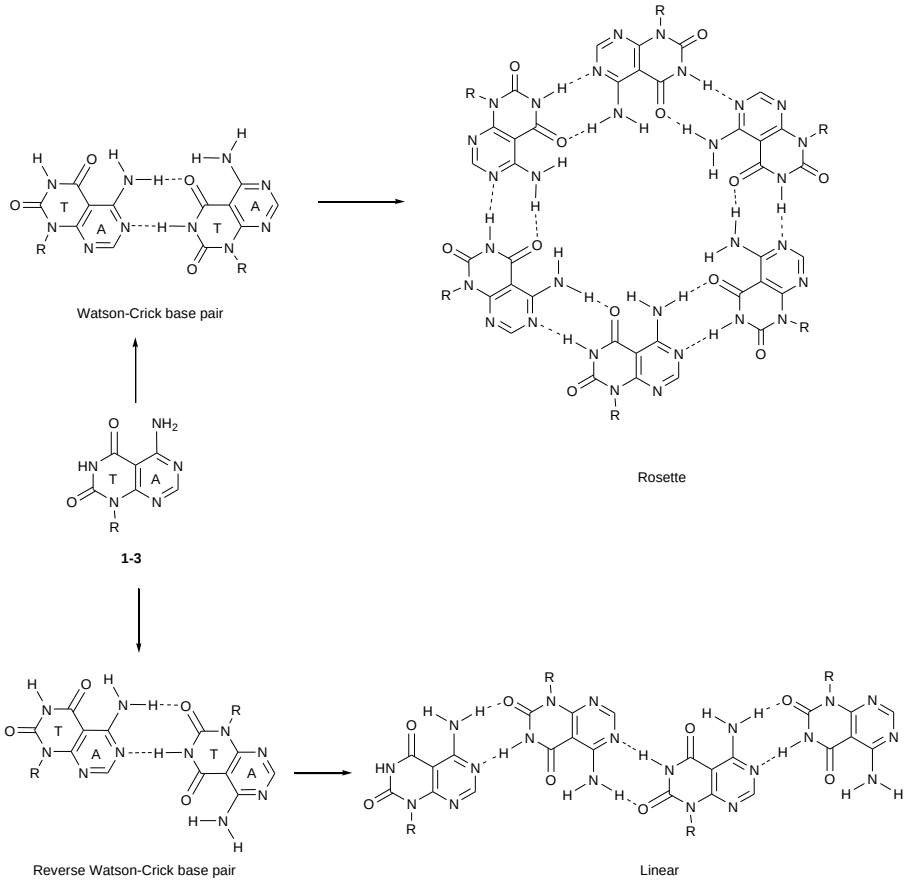

Scheme S4. Base pair motifs of J-TA nucleosides (**1**-**3**).

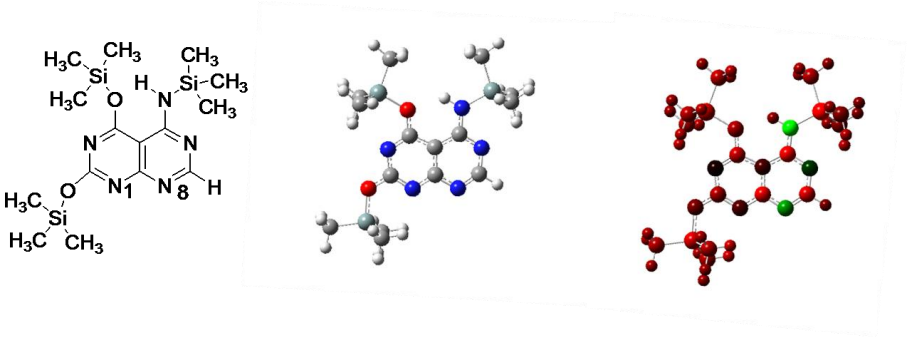

(a) **(b)** **(c)**

Figure S1. Reactivity of N8 in compound **5**. (a) and (b) Stucture of compound **5**. (c) Atomic nucleophilic fukui functions. The fukui functions were computed differentially the changes in atomic net charge of neutral and cationic molecules[S7]. Natural bond orbital (NBO) analysis[S8] was used to evaluate atomic charges (NPA charge). In this way, the nucleophilic fukui functions were computed and scaled with colors in (c). From red to green fukui function increases and denotes stronger nucleophilic reactivity.

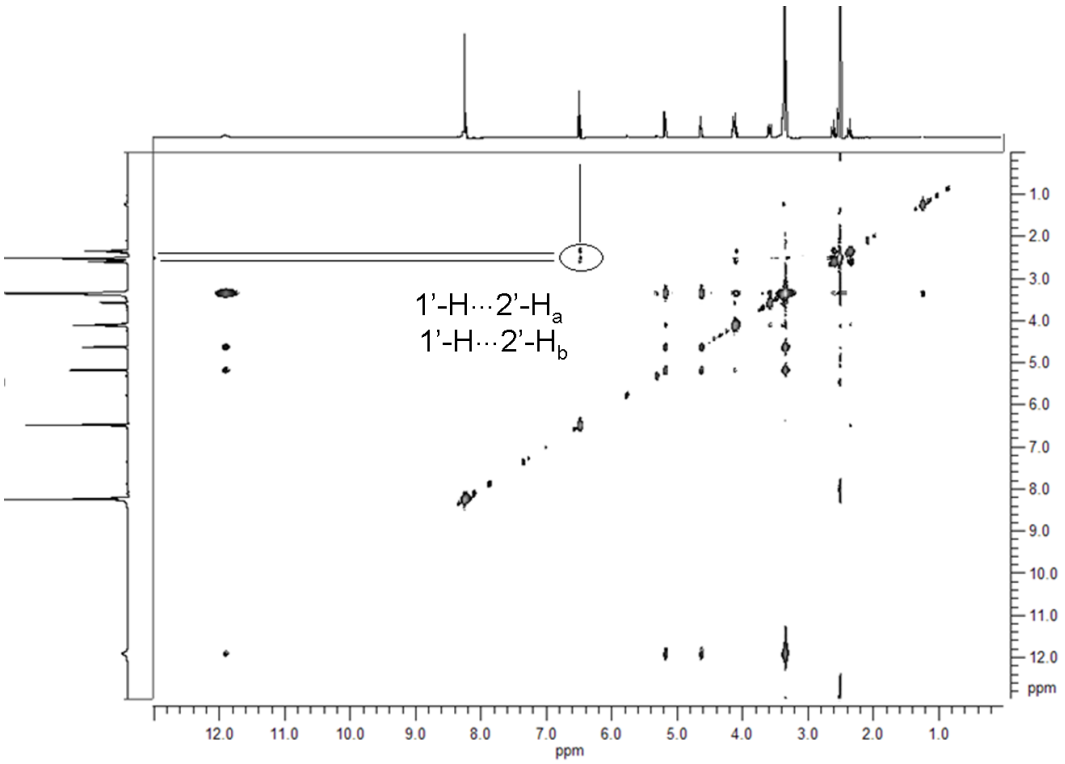

Figure S2. The NOE NMR spectra for compound **2.**

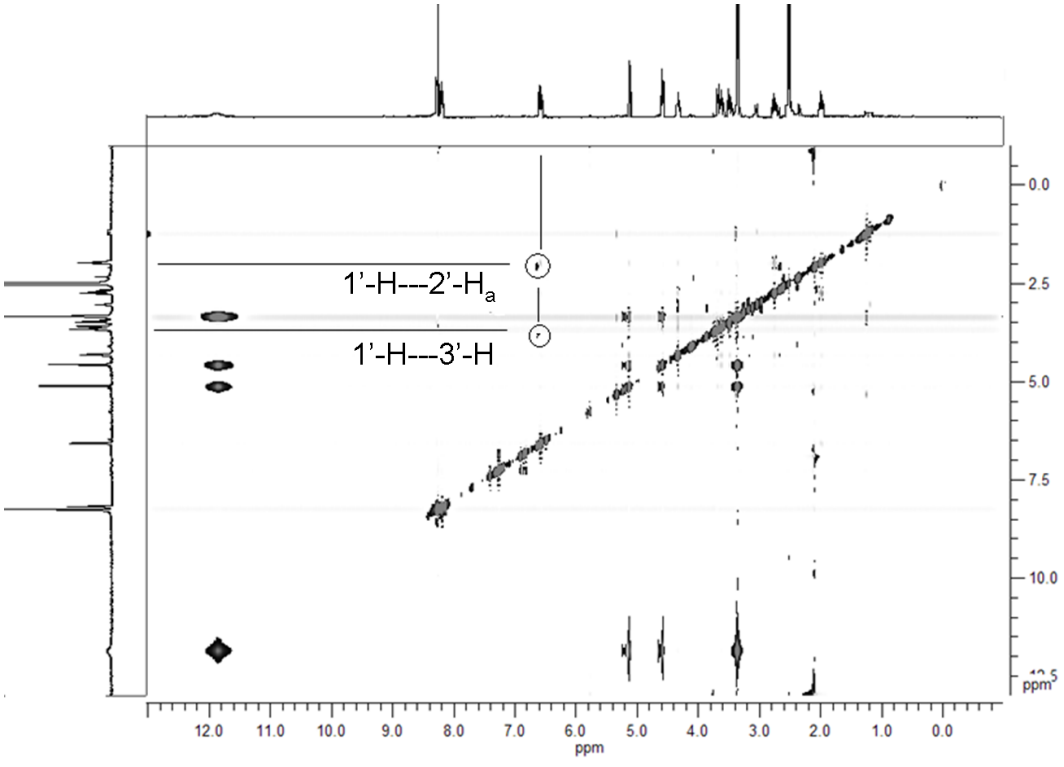

Figure S3. The NOE NMR spectra for compound **3.**

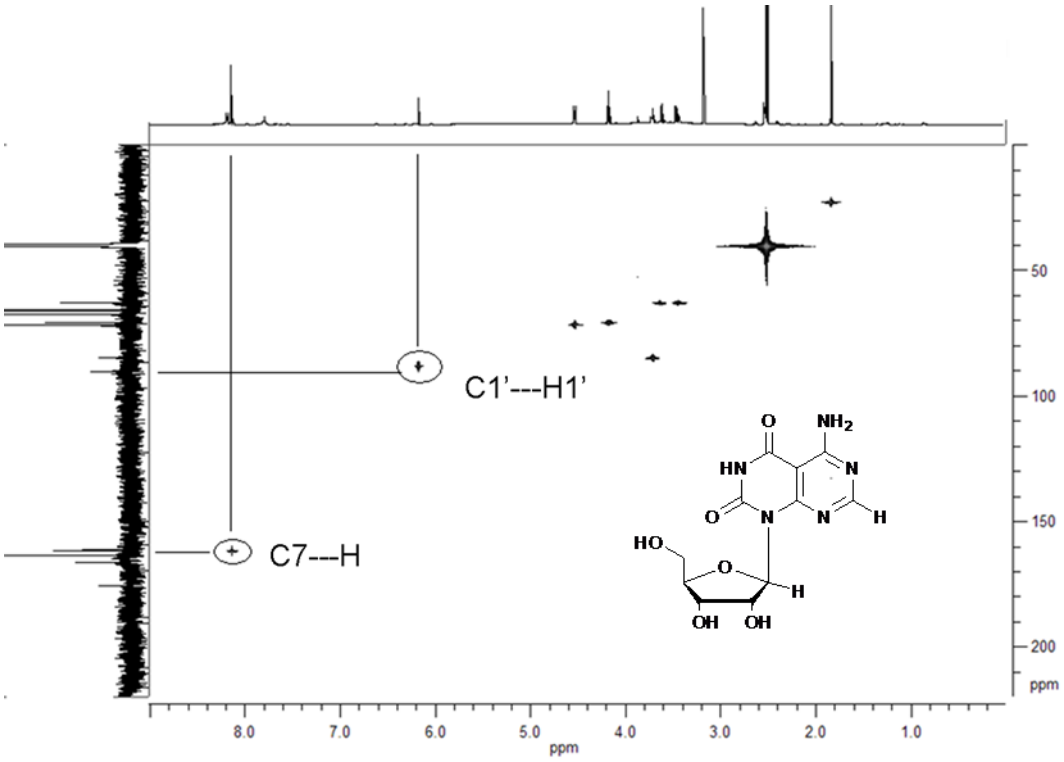

Figure S4. The HMQC NMR spectra for compound **1.**

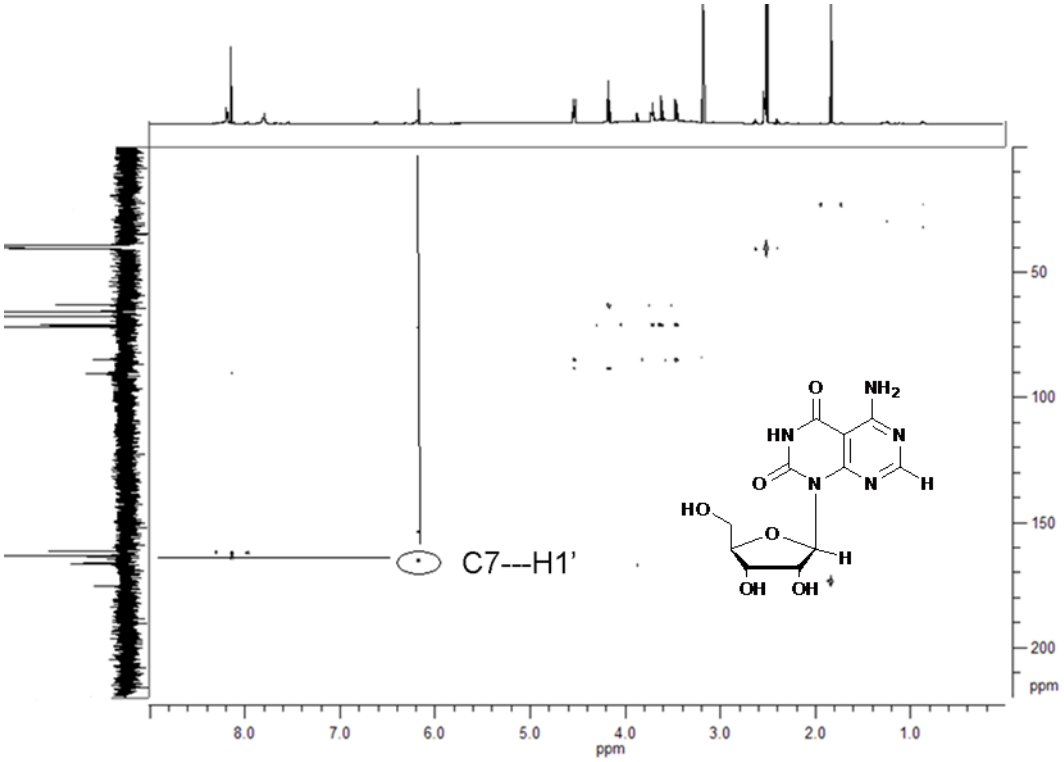

Figure S5. The HMBC NMR spectra for compound **1.**

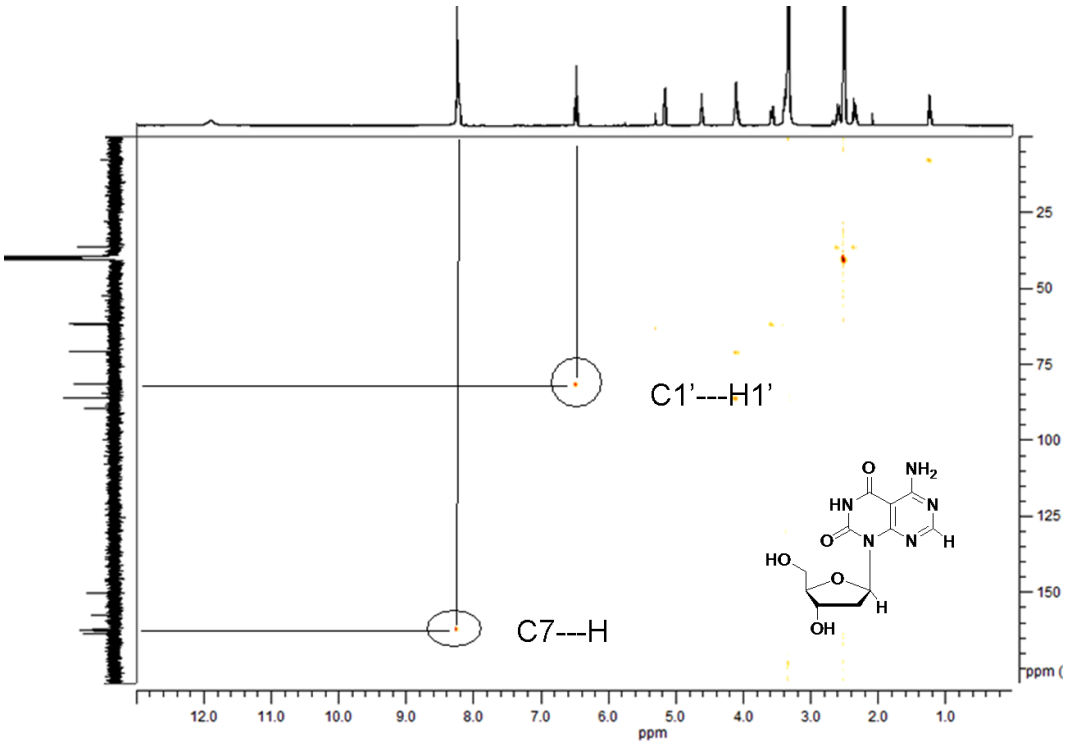

Figure S6. The HMQC NMR spectra for compound **2.**

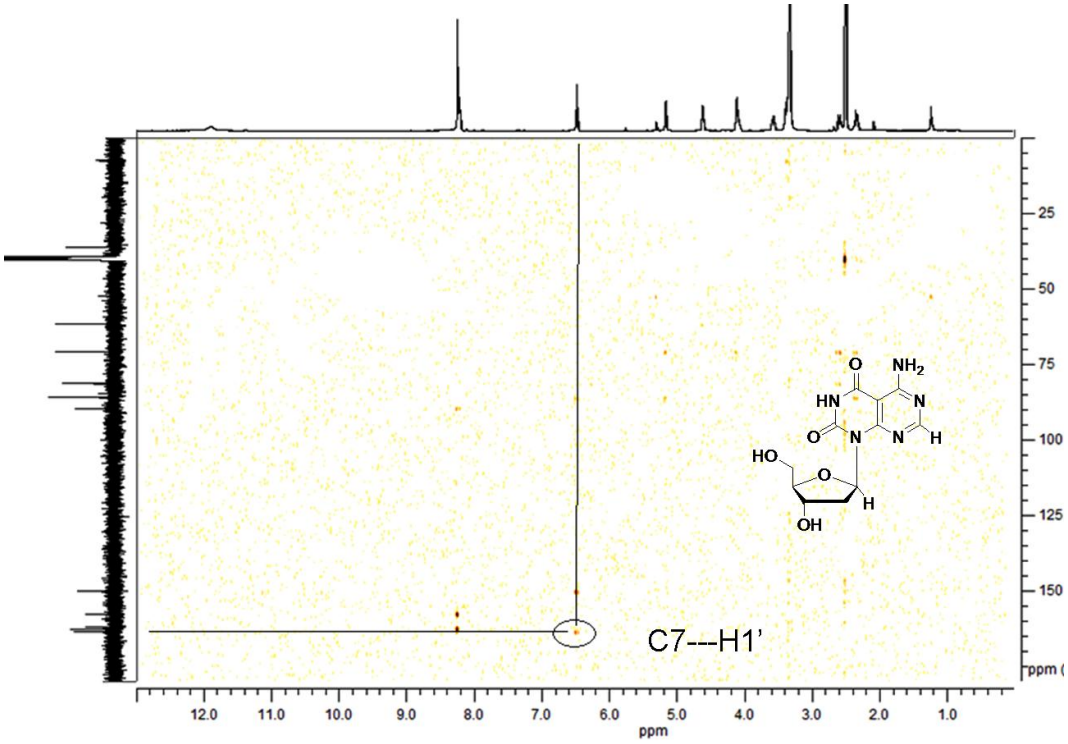

Figure S7. The HMBC NMR spectra for compound **2.**

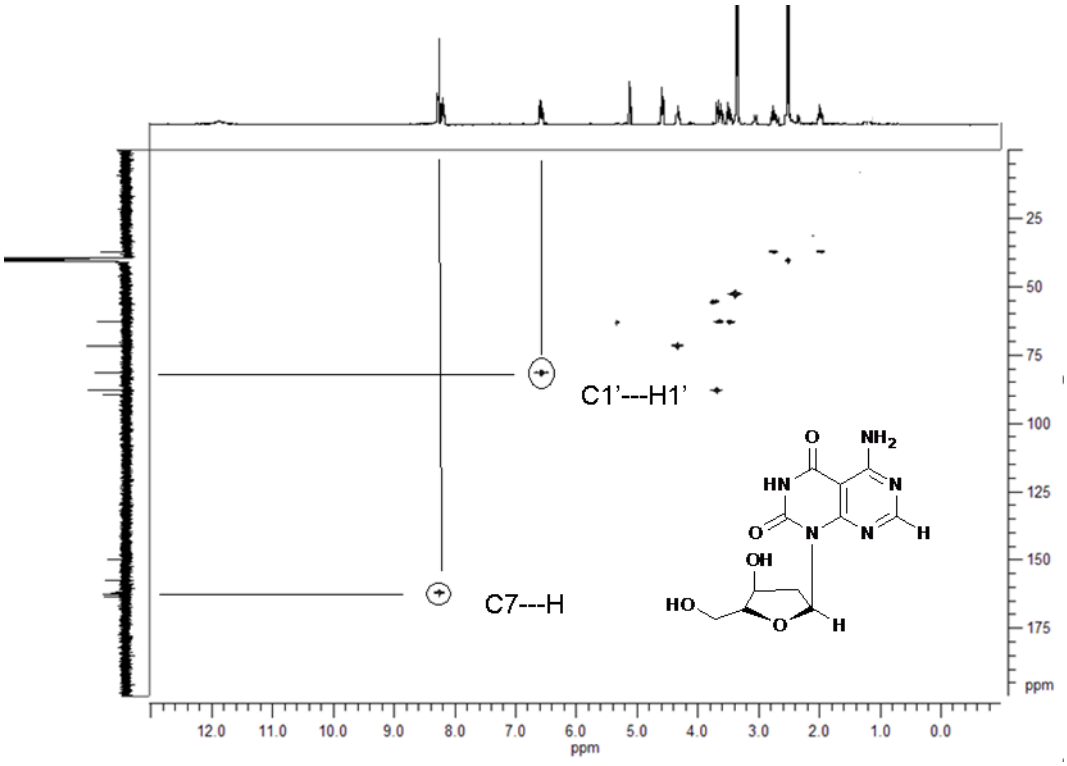

Figure S8. The HMQC NMR spectra for compound **3.**

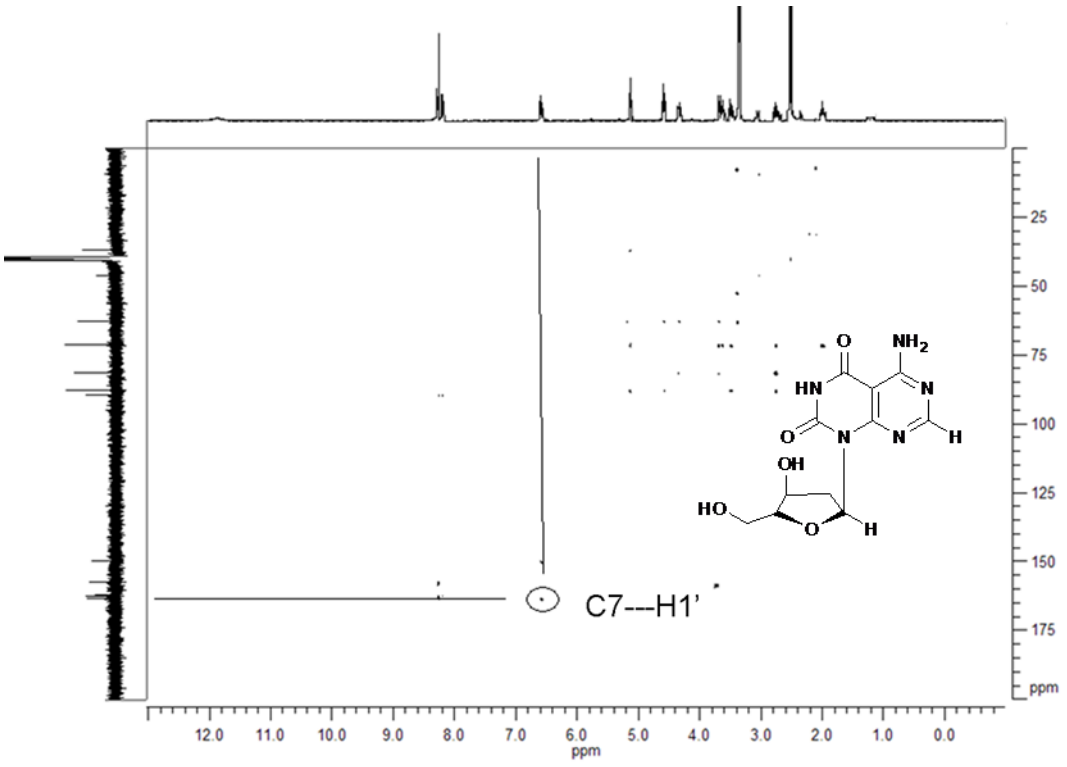

Figure S9. The HMBC NMR spectra for compound **3.**

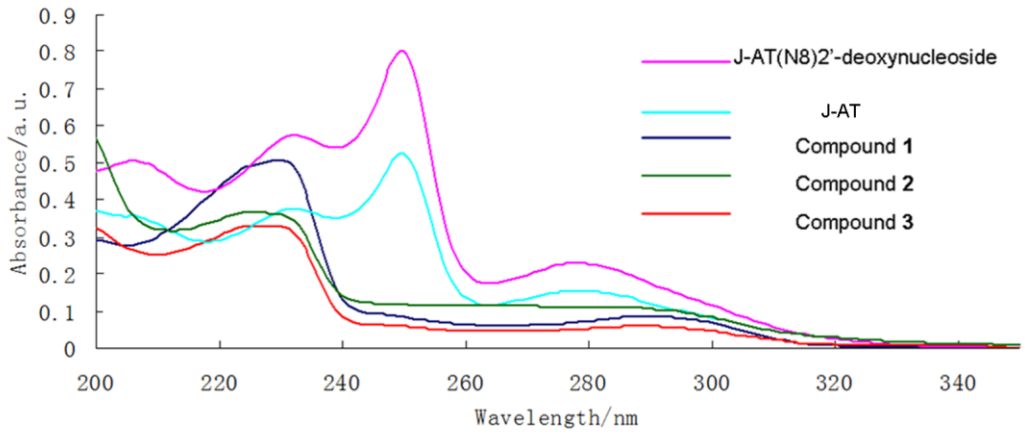

Figure S10 . The UV spectra of compounds (**1-3**), J-AT and J-AT (N8) 2'-deoxynucleoside. The J-AT ribose nucleoside and its 2'-deoxyribose nucleoside had absorbance maximum at 250 nm; the absorbance maximum of nucleosides **1-3** was blue shifted to 227 nm, due to their different isomeric form from J-AT.

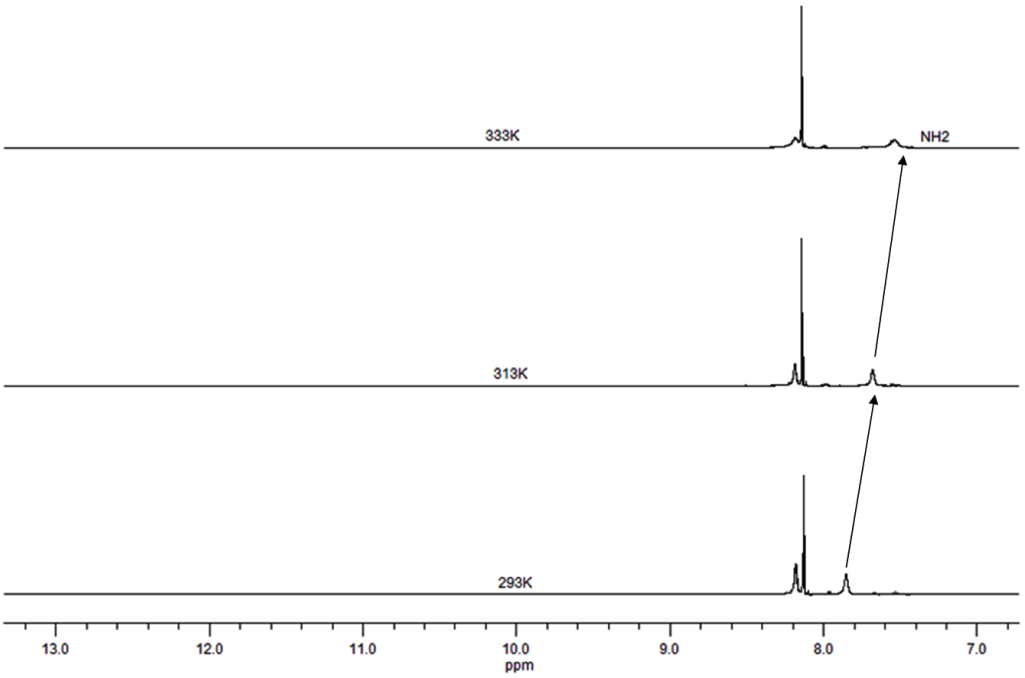

Figure S11. The variable temperature ^{1}HNMR spectra of compound **1**. The chemical shift for N11H atom of the amino group on the adenine ring moving from δ 7.85 (293 K) to δ 7.51 ppm (333 K) with Δδ = 0.34 ppm, the result showed that the hydrogen atoms (N11H) were involved in the formation of intermolecular hydrogen-bond; and another NH atom from the amino group on the adenine ring at 8.18 ppm was assigned to be the intramolecular hydrogen-bond since the chemical shift remains unchanged.

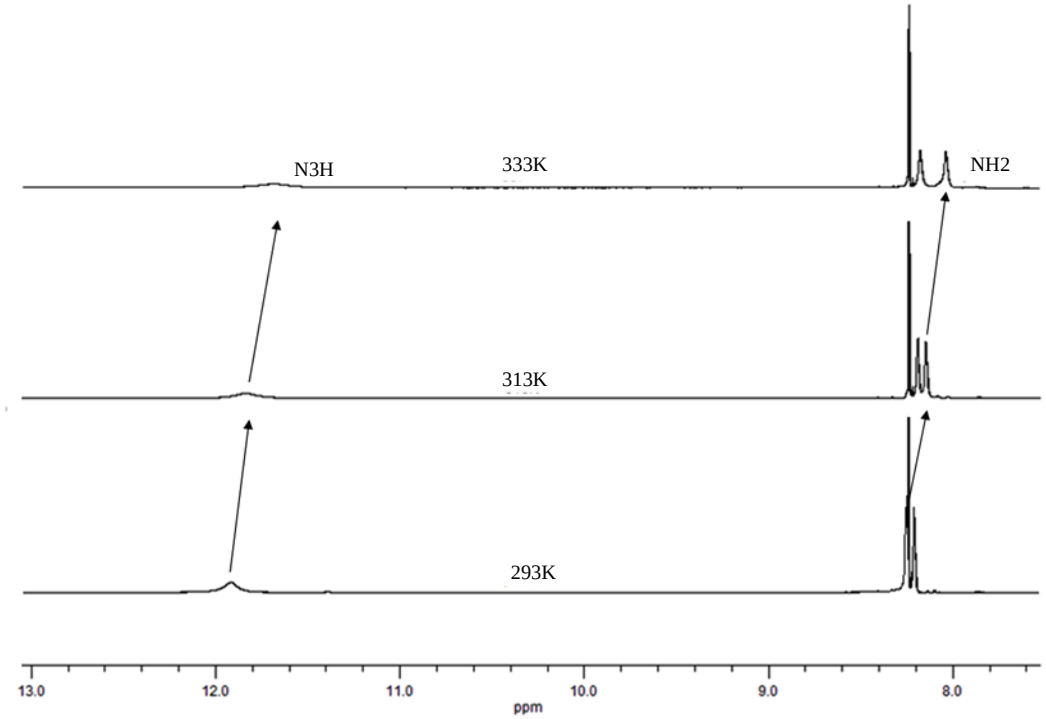

Figure S12. The variable temperature ^{1}HNMR spectra of compound **2**. The chemical shift of the hydrogen atom of imino group on the thymine ring (N3H) moved upon temperature elevation, from δ 11.92 (293 K) to 11.74 ppm (333 K) with Δδ = 0.18 ppm; and the chemical shift for N11H atom of the amino group on the adenine ring moved from δ 8.25 (293 K) to δ 8.04 ppm (333 K) with Δδ = 0.21 ppm. These results showed that these hydrogen atoms (N3H and N11H) were involved in the formation of intermolecular hydrogen-bonds. The chemical shift of the other hydrogen atom (δ 8.24 ppm) of the amino group on the adenine ring participating in the intramolecular hydrogen bond remains unchanged upon the temperature increasing.

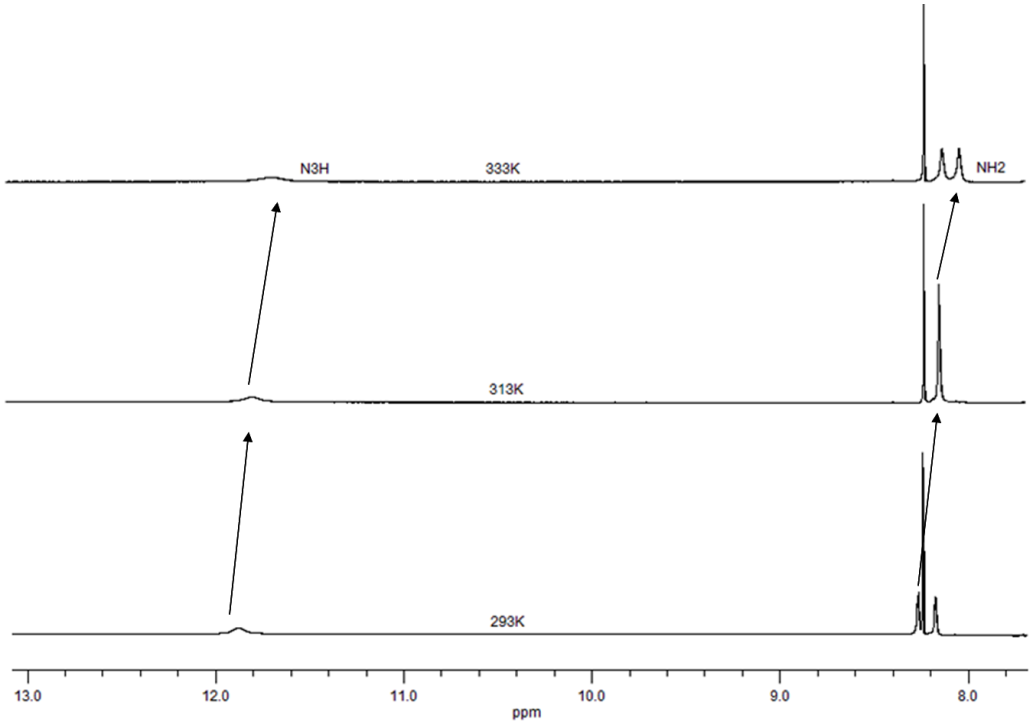

Figure S13. The variable temperature ^{1}HNMR spectra of compound **3**. The similar intermolecular hydrogen-bond of compound **2** were observed, with $\Delta\delta$ = 0.19 ppm (from 293 K to 333 K) for N3H and $\Delta\delta$ = 0.21 ppm (from 293 K to 333 K) for the N11H atom of the amino group on the adenine ring. The other hydrogen atom (δ 8.24 ppm) in amino group on the adenine ring participating in the intramolecular hydrogen bond remains unchanged upon the temperature rising.

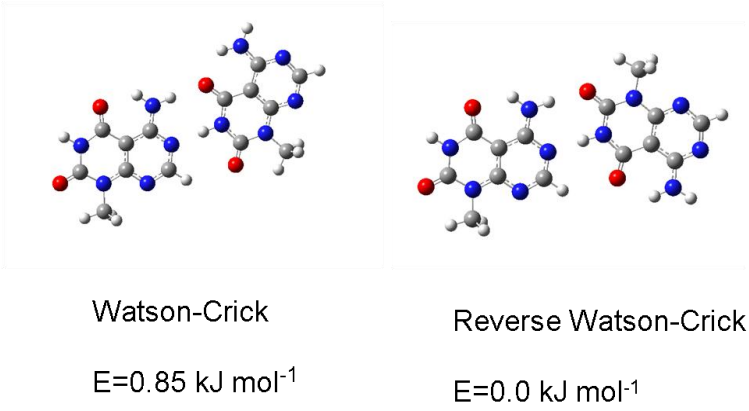

Figure S14. Structures of WC and RWC base pairs. Very small energy difference (0.85 kJ mol^{-1}) was predicted between them at M062X/6-31G(d,p) level.

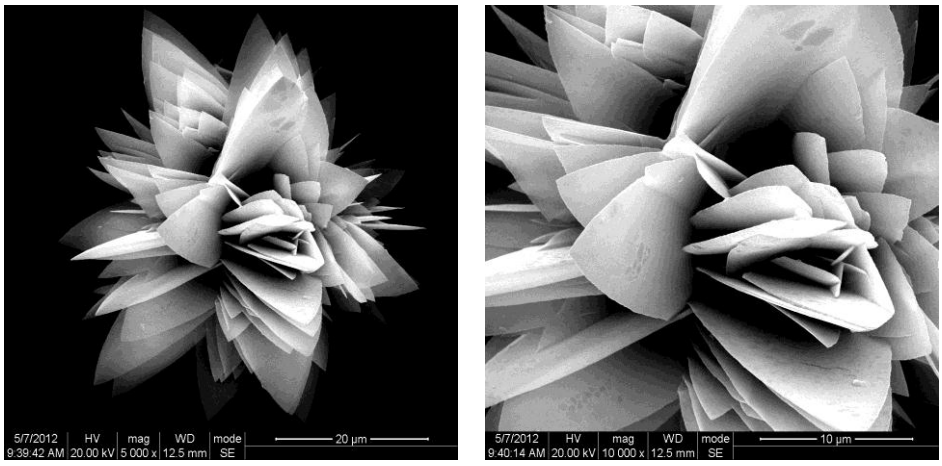

Figure S15. SEM images of J-AT (0.2 mg mL^{-1} in H_2O) recorded on INSPECT F50.

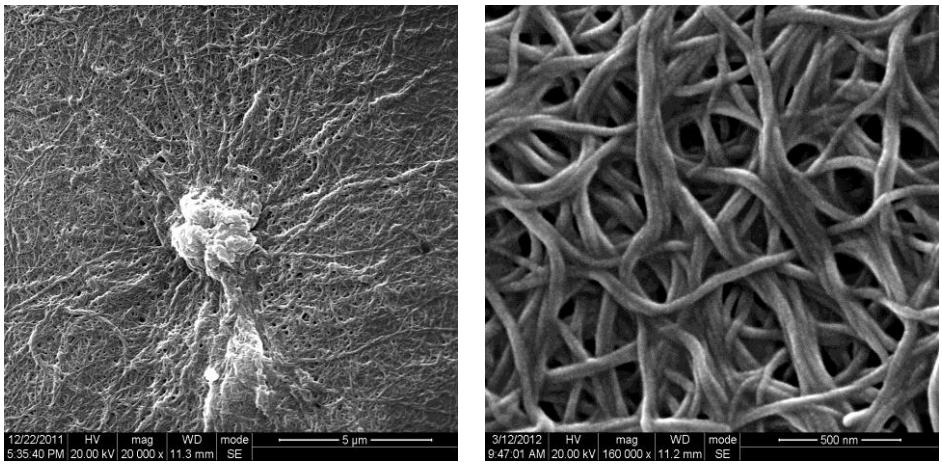

Figure S16. SEM images of compound **1** (0.2 mg mL^{-1} in H_2O) recorded on INSPECT F50.

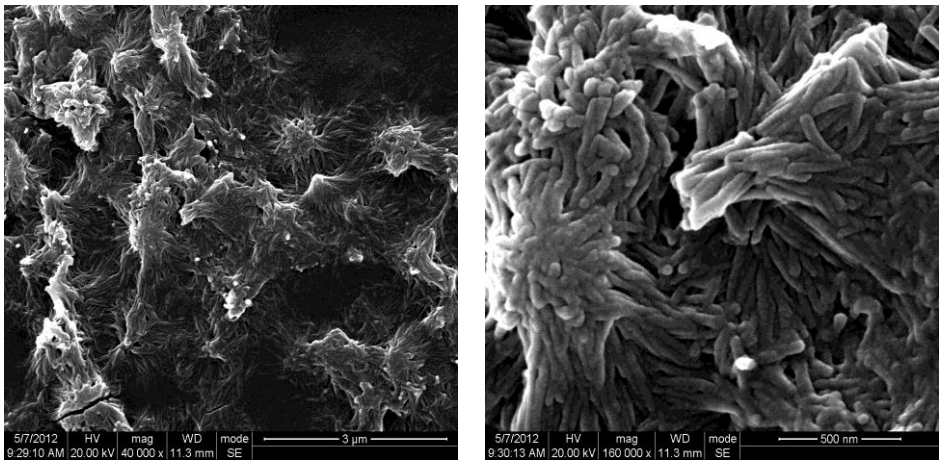

Figure S17. SEM images of compound **2** (0.2 mg mL^{-1} in H_2O) recorded on INSPECT F50.

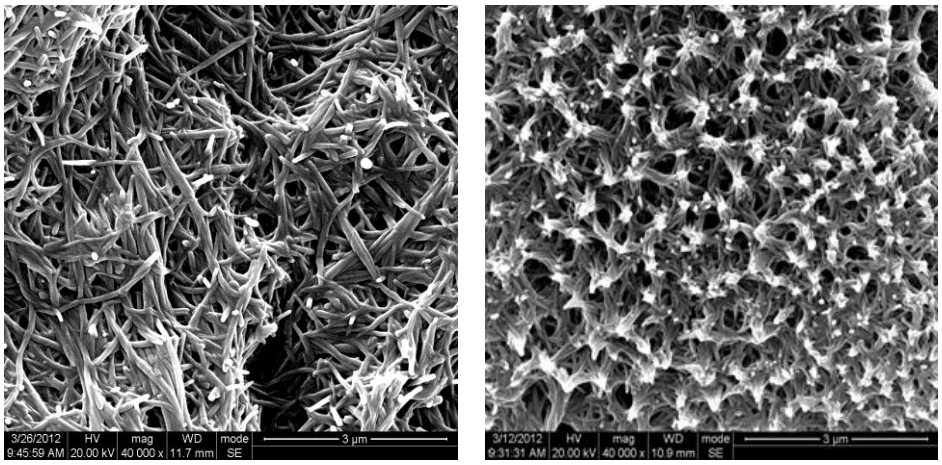

Figure S18. SEM images of compound **3** (0.2 mg mL^{-1} in H_2O) recorded on INSPECT F50.

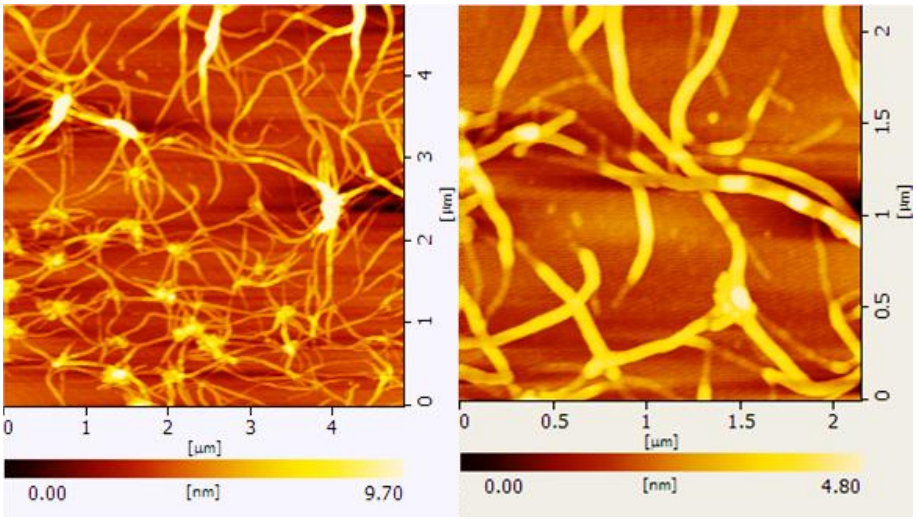

Figure S19. TM–AFM height and amplitude images of compound **1** (0.2 mg mL^{-1} in H_2O).

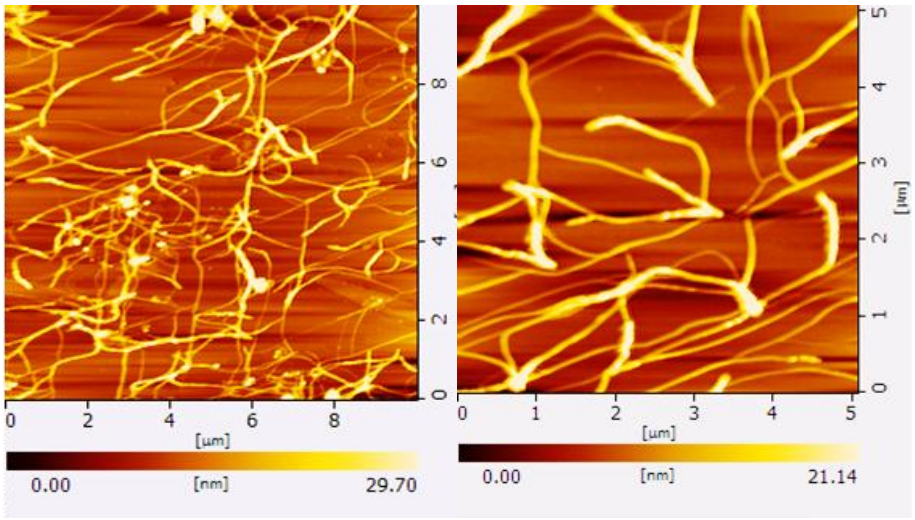

Figure S20. TM–AFM height and amplitude images of compound **2** (0.2 mg mL^{-1} in H_2O).

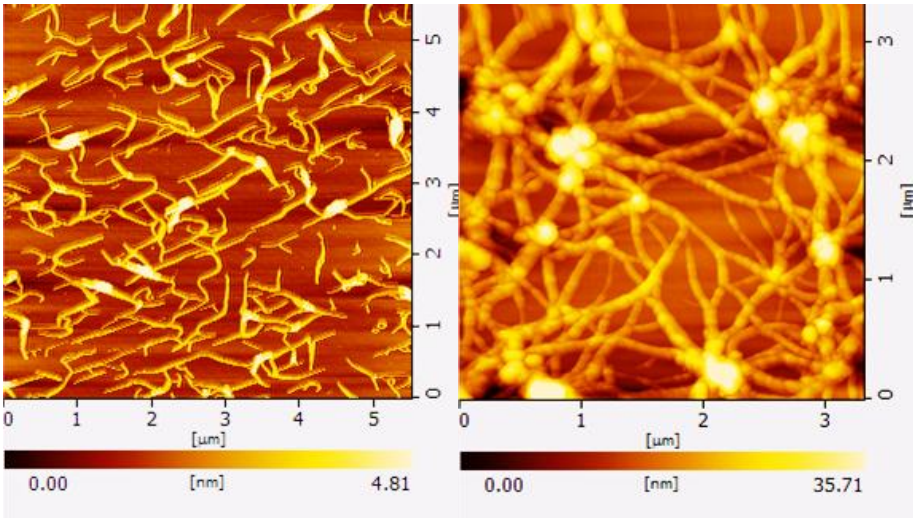

Figure S21. TM–AFM height and amplitude images of compound **3** (0.2 mg mL^{-1} in H_2O).

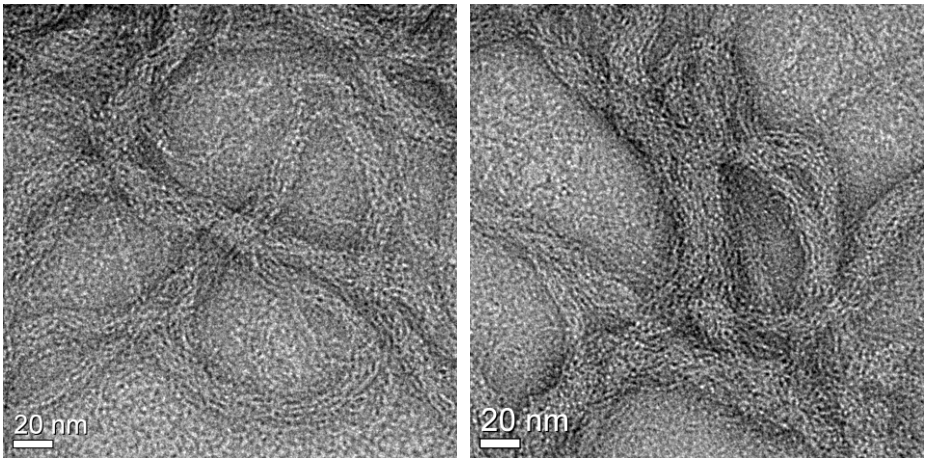

Figure S22. TEM images of compound **1**.

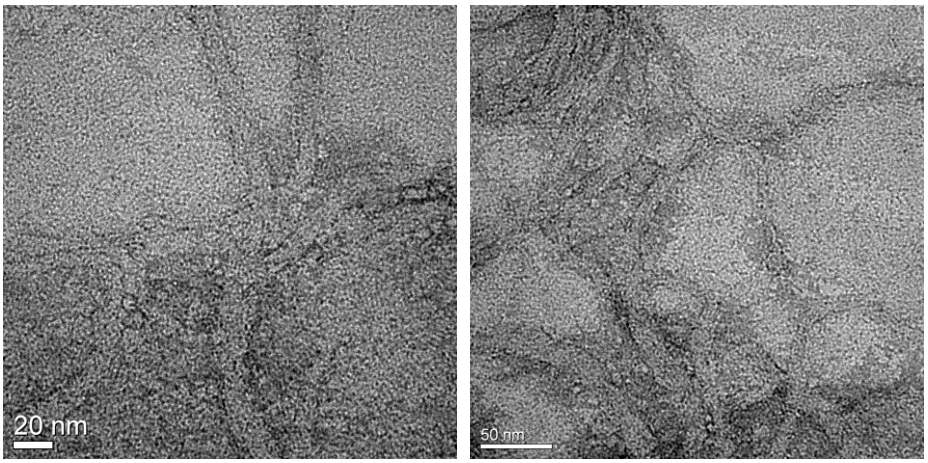

Figure S23. TEM images of compound **2**.

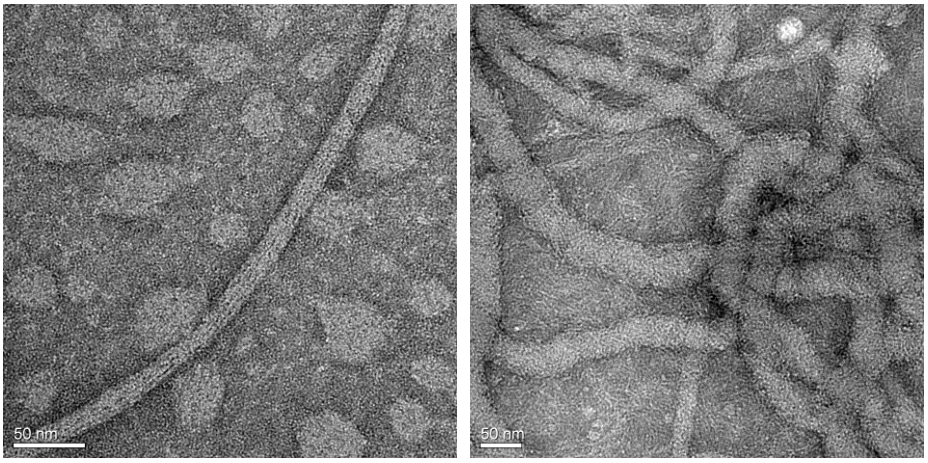

Figure S24. TEM images of compound **3**.

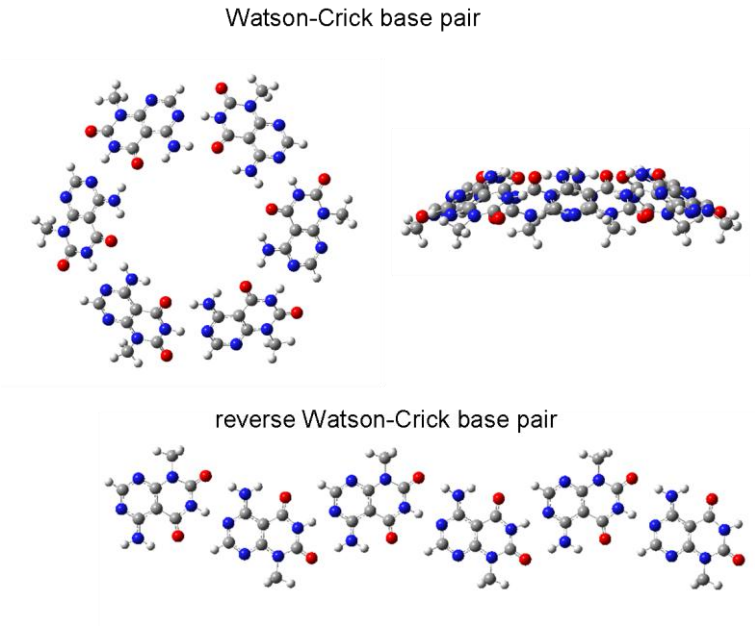

Figure S25. Structures of WC (upper) and RWC (lower) hexamers. A cyclic structure is formed for the former and a linear structure for the latter. The cyclic structure is 43.05 kJ mol^{-1} more stable than the linear one at M062X/6-31G(d,p) level.

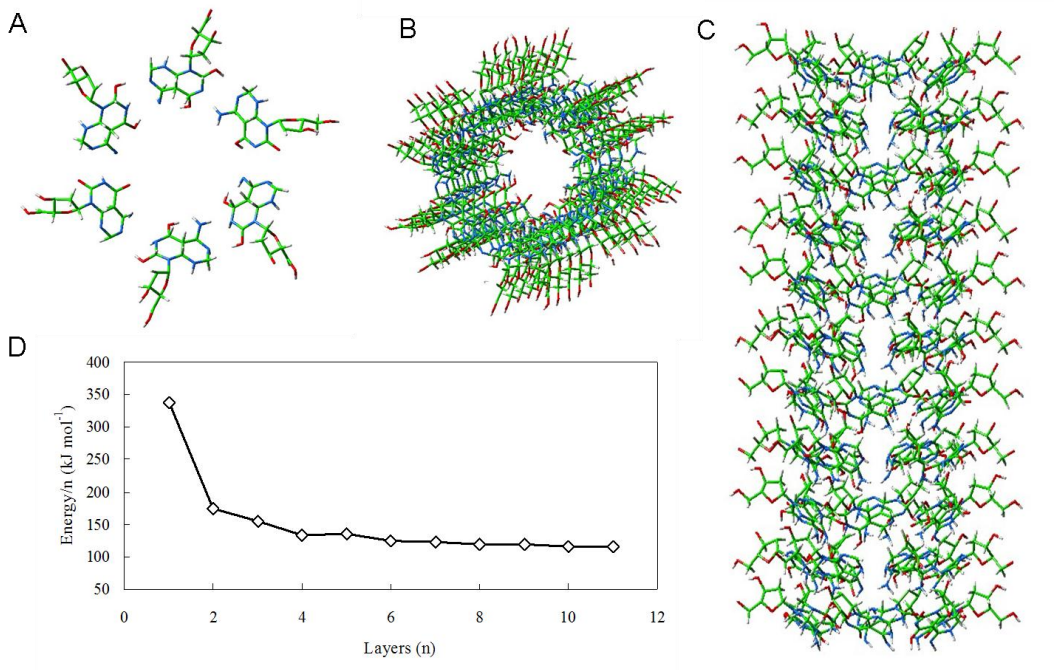

Figure S26. Stacking of cyclic J-TA hexamers. (A) Structure of a J-TA hexamer (one layer); (B) Top view of stacked J-TA hexamers; (C) Side view of stacked J-TA hexamers (11 layers); (D) Variation of energy per layer (E/n) with layers (n). E/n tends to decrease with n increase, indicating that the stacking stabilizes the hexamers and favors the formation of J-TA nanotube.

References

S1 Y. Zhao, N. E. Schultz, and D. G. Truhlar, *J. Chem. Phys.* 2005, **123**, 1.

S2 Gaussian 03W, M. J. Frisch, G. W. Trucks, H. B. Schlegel, G. E. Scuseria, M. A. Robb, J. R. Cheeseman, J. A. Montgomery, Jr. T. Vreven, K. N. Kudin, J. C. Burant, J. M. Millam, S. S. Iyengar, J. Tomasi, V. Barone, B. Mennucci, M. Cossi, G. Scalmani, N. Rega, G. A. Petersson, H. Nakatsuji, M. Hada, M. Ehara, K. Toyota, R. Fukuda, J. Hasegawa, M. Ishida, T. Nakajima, Y. Honda, O. Kitao, H. Nakai, M. Klene, X. Li, J. E. Knox, H. P. Hratchian, J. B. Cross, C. Adamo, J. Jaramillo, R. Gomperts, R. E. Stratmann, O. Yazyev, A. J. Austin, R. Cammi, C. Pomelli, J. W. Ochterski, P. Y. Ayala, K. Morokuma, G. A. Voth, P. Salvador, J. J. Dannenberg, V. G. Zakrzewski, S. Dapprich, A. D. Daniels, M. C. Strain, O. Farkas, D. K. Malick, A. D. Rabuck, K. Raghavachari, J. B. Foresman, J. V. Ortiz, Q. Cui, A. G. Baboul, S. Clifford, J. Cioslowski, B. B. Stefanov, G. Liu, A. Liashenko, P. Piskorz, I. Komaromi, R. L. Martin, D. J. Fox, T. Keith, M. A. Al-Laham, C. Y. Peng, A. Nanayakkara, M. Challacombe, P. M. W. Gill, B. Johnson, W. Chen, M. W. Wong, C. Gonzalez, and J. A. Pople, Gaussian, Inc. Pittsburgh PA, 2003.

S3 J. Tomasi, B. Mennucci, and R. Cammi, *Chem. Rev.* 2005, **105**, 2999.

S4 S. Simon, M. Duran, and J. J. Dannenberg, *J. Chem. Phys.* 1996, **105**, 11024.

S5 Piotr Cieplak, James Caldwell and Peter Kollman, *Journal of Computational Chemistry*, 2001, **22**, 1048.

S6 D. A. Case, T. A. Darden, T. E. Cheatham, C. L. Simmerling, J. Wang, R. E. Duke, R. Luo, K. M. Merz, D. A. Pearlman, M. Crowley, R. C. Walker, W. Zhang, B. Wang, S. Hayik, A. Roitberg, G. Seabra, K. F. Wong, F. Paesani, X. Wu, S. Brozell, V. Tsui, H. Gohlke, L. Yang, C. Tan, J. Mongan, V. Hornak, G. Cui, P. Beroza, D. H. Mathews, C. Schafmeister, W. S. Ross, and P. A. Kollman 2006, AMBER 9, University of California, San Francisco.

S7 P. Geerlings, F. De Proft,and W. Langenaeker. *Chem. Rev.* 2003**, 103**, 1793.

S8 A. E. Reed, L. A. Curtiss, and F. Weinhold, *Chem. Rev.* 1988, 899.